Physalin A alleviates intervertebral disc degeneration via anti-inflammatory and anti-fibrotic effects

Rui Lu [a],[1], Haoran Xu [a],[1], Xiaofeng Deng [b], Yingguang Wang [a], Zhiyi He [a], Shimeng Xu [a], Shuang Liang [a], Xiaojian Huang [a], Hongbo You [a], Fengjing Guo [a], Peng Cheng [a],[*], An-min Chen [a],[**]

[a] Department of Orthopedics, Tongji Hospital, Tongji Medical College, Huazhong University of Science and Technology, Wuhan, 430030, China
[b] Department of Rehabilitation, Tongji Hospital, Tongji Medical College, Huazhong, University of Science and Technology, Wuhan, 430030, China

ARTICLE INFO

ABSTRACT

Background: The incidence of intervertebral disc degeneration (IVDD) is a common degenerative disease with inflammation, decreased autophagy, and progression of fibrosis as its possible pathogenesis. Physalin A (PA) is a widely studied anti-inflammatory drug. However, its therapeutic effects on IVDD remain unexplored. Therefore, we aimed to explore the therapeutic potential of PA in IVDD progression.

Materials and methods: In vivo, we investigated PA bioactivity using a puncture-induced IVDD rat model. IVDD signals and height changes were detected using X-ray, micro-CT, and MRI, and structural and molecular lesions using histological staining and immunohistochemistry of intervertebral disc sections. In vivo, interleukin-1 beta (IL-1β) and TGF-β1 were employed to establish inflammation fibrotic nucleus pulposus (NP) cells. The PA effect duration, concentration, influence pathways, and pathological changes in IVDD treatment were elucidated using western blotting, real-time PCR, and immunofluorescence.

Results: PA exerted significant effects on IVDD remission due to anti-inflammation, fibrosis reduction, and autophagy enhancement. In vitro, PA improved inflammation by blocking the NF-κB and MAPK pathways, whereas it promoted autophagy via the PI3K/AKT/mTOR pathway and affected fibrotic progression by regulating the SMAD2/3 pathway. Moreover, PA improved the disc degeneration process in IVDD model.

Conclusions: PA exhibited significant anti-inflammatory and anti-fibrotic effects and improved autophagy in *vivo* and *in vitro* IVDD models, thus effectively relieving IVDD progression, indicating it is a promising agent for IVDD treatment.

The translational potential of this article: This study successfully reveals that PA, a natural bioactive withanolide, effectively relieved IVDD progression via inflammation inhibition, fibrosis reduction, and autophagy enhancement, indicating it is a promising agent for IVDD treatment.

1. Introduction

The intervertebral disc (IVD) comprises the nucleus pulposus (NP), annulus fibrosus, and endplate cartilage, which exert several physiological functions, including absorbing shock, transmitting and buffering load, and maintaining spinal movement. Intervertebral disc degeneration (IVDD) is a gradual process that is mainly responsible for the development of that is mainly responsible for IVD herniation and other spinal

diseases. IVDD is the most common cause of neck and lower back pain [1], also accompanied by pain, numbness, and sensory and motor abnormalities in the upper or lower extremities [2]. IVDD affects approximately 60–80% of the global population, thereby causing a heavy social and economic burden [3]. However, the specific pathogenic mechanisms of IVDD have not been comprehensively elucidated yet.

Various factors such as the inflammatory environment [4,5], autoimmunity [6,7], autophagy [8], fibrosis [9], and mechanical load [10]

---

affect and mediate IVDD progression. Under the persistent influence of pathological mechanisms, NP cell extracellular matrix (ECM) causes degenerative phenotypic changes, including secretion of matrix metalloproteinases (MMPs) [11], various inflammatory mediators [12], and degeneration of aggrecan (Acan) and type II collagen (Col2a1) [13]. Modulating the associated pathogenesis to reverse the degenerative phenotype contributes to IVDD alleviation [14]. Inflammation is a crucial initiator that regulates IVDD pathophysiology, weakens anabolism, and enhances catabolism in NP cells [15]. The pathogenesis of inflammation in IVDD includes recruitment of inflammatory cells, secretion of inflammatory mediators and activation of inflammatory signaling pathways, which contribute to the NP cells degeneration [16,17]. Moreover, inflammation is associated with attenuated autophagy and enhanced fibrosis in process of degeneration [18,19]. According to previous studies, a variety of inflammatory cytokines such as IL-1β and TNF-α, stimulate the NP cells and lead to an impaired autophagy process [20]. Moreover, IL-1β as a key signal for leading to fibrogenesis, and related to regulating TGF-β generation [21]. Responsive to the stimulation of TGF-β1, NP cell fibrosis progression not only up-regulates fibrotic protein [α-smooth muscle actin (α-SMA) and type I collagen (Col1a1)] expression, leading to NP sclerosis and loss of elasticity, but also further promotes inflammation and accelerates IVDD deterioration [22]. Therefore, to break this vicious cycle, anti-inflammatory [23] and anti-fibrosis strategies [24] are pivotal during IVDD progression [23]. Thus, exploring new drugs to treat IVDD is imperative.

Physalin A (PA) is a natural bioactive withanolide extracted from *Physalis alkekengi* var. Franchetii that possesses several biological characteristics, such as anti-inflammatory [25,26], anti-oxidant [27], and anti-tumor [28,29] activities. In our previous study, PA had shown excellent chondroprotective effect by inhibiting MAPK and NF-κB signaling pathways, such as reducing inflammatory responses and recovering ECM degeneration [26]. These signaling pathways are thought to play crucial roles in IVDD onset and development. Furthermore, based on extensive researches, physalis-base drugs exert ideal anti-fibrotic abilities in diseases of other systems [30]. Therefore, PA may be an optimal and potential drug against the pathogenesis of disc degeneration and may improve IVDD progression. However, the therapeutic potential of PA in IVDD remains unclear.

Therefore, we hypothesized that PA treatment may reduce inflammation and fibrosis and promote autophagy to prevent IVDD progression. In herein, a puncture-induced IVDD model was used to evaluate the anti-degenerative effect of PA treatment on the disc. To elucidate the underlying mechanisms, we explored the effects of PA on inflammatory and fibrotic degeneration in an NP cell model via a series of *in vitro* experiments. In this study, we sought to demonstrate the anti-inflammatory, anti-fibrotic, and promote autophagy effects, which provide a theoretical basis for the clinical application of PA.

2. Methods

2.1. Experimental materials and reagents

PA (HY–N9942), dimethyl sulfoxide (DMSO, HY-Y0320) and TGF beta 1 (TGF-β1, HY-P70648) were purchased from MedChemExpress (Monmouth Junction, NJ, USA). Recombinant rat interleukin-1 beta (IL-1β) protein was purchased from R&D Systems (Minneapolis, USA).

2.2. Animals

Male Sprague-Dawley rats (6–8 weeks old, 220 ± 20 g) were obtained from Vital River Laboratories (Beijing, China). The rats were fed and tested under specific pathogen-free conditions. The *in vivo* experiments were conducted following the guidelines of the International Guiding Principles for Animal Research and approved by the Ethics Committee of Huazhong University of Science and Technology.

2.3. Cell harvest and culture

NP cells were harvested from the inner tissue of tail disc of Sprague-Dawley rats. After cutting and disinfecting, tail epidermis and tendons were separated and discs were exposed under sterile condition. NP tissues were collected and digested by 0.25% trypsin (37 °C, 30 min) and type II collagenase (37 °C, 3 h). The NP cells were cultured in DMEM/F12 medium (Hyclone, USA) supplemented with 10% fetal bovine serum (Gibco, USA) and 1% penicillin/streptomycin (Gibco, USA) in an incubator with 5% CO_2 at 37 °C.

2.4. Cell viability assay

To detect cell viability after treated with reagents (PA, IL-1β, and TGF-β1), the NP cells were seeded into 96-well plates (5×10^3 cells per well), three replicate wells were set up in each group. The NP cells were administrated with different IL-1β concentrations (0, 1, 2.5, 5, 10, and 20 ng/ml) for 48 h or time durations (5 ng/ml for 0, 3, 6, 12, 24, and 48 h) or 5 ng/ml IL-1β +/− 20 μM PA for 48 h or 10 ng/ml TGF-β1 +/− 20 μM PA for 48 h. Then Cell Counting Kit-8 (Vazyme Biotech, USA) was used to detect cell viability, and absorbance (wavelength of 450 nm) was evaluated using a microplate reader (BioTek, USA).

2.5. Western blot analysis

NP cell proteins were extracted and homogenized using RIPA buffer (Boster, China) containing 1% phosphatase and protease inhibitors (Boster, China). The BCA Protein Assay Kit (Boster, China) was used to determine the protein concentration. The protein samples (20 μg) were separated using SDS-PAGE and electrotransferred to a 0.45-μm PVDF membrane (Millipore, USA). Membranes were blocked with 5% bovine serum albumin (BSA; BioFroxx, Germany) for 1 h and incubated with the primary antibodies listed in Table 1 overnight at 4 °C. The next day, the membranes were immunoblotted with the corresponding secondary antibodies (Boster, China) at room temperature for 1 h and visualized using SuperSignal West Pico Chemiluminescent Substrate (Thermo Scientific, USA). The signal from the blots was detected and analyzed using the ChemiDoc Xrs Imaging System (BIO-RAD, USA).

2.6. RT-qPCR analysis

Total NP cell RNA was extracted using TRIzol (Takara Bio Inc, Japan) and reverse transcribed to cDNA using the PrimeScript 1st Strand cDNA Synthesis Kit (Toyobo, Japan). The cDNA was amplified using SYBR Premix Ex Tap (Toyobo, Japan), and specific primers (Table 2). Gene expression levels were revealed from fluorescence signals detected by the RT-PCR detection system (Bio-Rad Laboratories, USA). The mRNA expression levels of target genes were normalized to GAPDH expression levels and analyzed using the $2^{-\Delta\Delta Ct}$ method.

2.7. Immunofluorescence (IF) analysis

NP cells were seeded into 24 well-plates (1×10^4 cells per well) and received different treatments after cell adhesion. At the endpoint, the cells were fixed with 4% paraformaldehyde (PFA; Servicebio, China) and permeabilized with 0.1% Triton X-100 (BioFroxx, Germany). After blocking with BSA for 1 h, the cells were incubated overnight at 4 °C with the primary antibodies listed in Table 3. The following day, the cells were incubated with the corresponding fluorescent secondary antibodies (Boster, China) at room temperature in the dark for 1 h and stained with DAPI (Boster, China) for 10 min. Immunofluorescence images were captured using a microscope (EVOS fl auto, Thermo Fisher Scientific, USA) and analyzed using ImageJ software (National Institutes of Health, USA).

Table 1
Primary antibodies for western bolt.

Primary Antibody	Catalog Number	Dilution Ratio	Source
GAPDH	60004-1-Ig	1:50,000	Proteintech Group, Wuhan, Hubei, China
Acan	13880-1-AP	1:1000	Proteintech Group, Wuhan, Hubei, China
Col2a1	28459-1-AP	1:1000	Proteintech Group, Wuhan, Hubei, China
MMP3	17873-1-AP	1:500	Proteintech Group, Wuhan, Hubei, China
MMP9	10375-2-AP	1:500	Proteintech Group, Wuhan, Hubei, China
MMP13	18165-1-AP	1:1000	Proteintech Group, Wuhan, Hubei, China
TGF-β1	21898-1-AP	1:1000	Proteintech Group, Wuhan, Hubei, China
IL-6	A14687	1:500	ABclonal, Wuhan, Hubei, China
COX-2	# 12,282	1:1000	Cell Signaling Technology, Beverly, MA, USA
Col1a1	# 84,336	1:1000	Cell Signaling Technology, Beverly, MA, USA
IL-1β	#12242	1:1000	Cell Signaling Technology, Beverly, MA, USA
iNOS	#13120	1:1000	Cell Signaling Technology, Beverly, MA, USA
p-SMAD2/3	#8828	1:1000	Cell Signaling Technology, Beverly, MA, USA
SMAD2/3	#8685	1:1000	Cell Signaling Technology, Beverly, MA, USA
α-SMA	#19245	1:1000	Cell Signaling Technology, Beverly, MA, USA
p-PI3K	#4228	1:1000	Cell Signaling Technology, Beverly, MA, USA
PI3K	#4229	1:1000	Cell Signaling Technology, Beverly, MA, USA
p-AKT	66444-1-Ig	1:2000	Proteintech Group, Wuhan, Hubei, China
AKT	60203-2-Ig	1:5000	Proteintech Group, Wuhan, Hubei, China
p-mTOR	67778-1-Ig	1:2000	Proteintech Group, Wuhan, Hubei, China
mTOR	66888-1-Ig	1:5000	Proteintech Group, Wuhan, Hubei, China
Atg3	#3415	1:1000	Cell Signaling Technology, Beverly, MA, USA
Atg7	#8558	1:1000	Cell Signaling Technology, Beverly, MA, USA
P62	18420-1-AP	1:1000	Proteintech Group, Wuhan, Hubei, China
Beclin-1	#3495	1:1000	Cell Signaling Technology, Beverly, MA, USA
LC3 I/II	#12741	1:1000	Cell Signaling Technology, Beverly, MA, USA
p-P38	#4511	1:1000	Cell Signaling Technology, Beverly, MA, USA
P38	#8690	1:1000	Cell Signaling Technology, Beverly, MA, USA
p-ERK	#4377	1:1000	Cell Signaling Technology, Beverly, MA, USA
ERK	#4695	1:1000	Cell Signaling Technology, Beverly, MA, USA
p-JNK	#4668	1:1000	Cell Signaling Technology, Beverly, MA, USA
JNK	#9252	1:1000	Cell Signaling Technology, Beverly, MA, USA
p-IKKα/β	#2697	1:1000	Cell Signaling Technology, Beverly, MA, USA
IKKα	#61294	1:1000	Cell Signaling Technology, Beverly, MA, USA
IKKβ	#8943	1:1000	Cell Signaling Technology, Beverly, MA, USA
p-IκBα	#2859	1:1000	Cell Signaling Technology, Beverly, MA, USA
IκBα	#4814	1:1000	Cell Signaling Technology, Beverly, MA, USA
p-P65	#3033	1:1000	Cell Signaling Technology, Beverly, MA, USA
P65	#8242	1:1000	Cell Signaling Technology, Beverly, MA, USA

Table 2
Primer sequence used in the RT-qPCR experiment.

Gene	RNA sequence
Rat-*Acan*-F	5′-CTTCCCAACTATCCAGCCAT-3′
Rat-*Acan*-R	5′-TCACACCGTATAGATCCCAGA-3′
Rat-*Col1a1*-F	5′-CGTGGAAACCTGATGTATGC-3′
Rat-*Col1a1*-R	5′-GGTTGGGACAGTCCAAGTCT-3′
Rat-*Col2a1*-F	5′-CGAGGCAGACAGTACCTTG-3′
Rat-*Col2a1*-R	5′-TGCTCTCGATCTGGTTGTTC-3′
Rat-*MMP3*-F	5′-GCTCATCCTACCCATTGCAT-3′
Rat-*MMP3*-R	5′-GCTTCCCTGTCATCTTCAGC-3′
Rat-*MMP9*-F	5′-TCCTTGCAATGTGGATGTTT-3′
Rat-*MMP9*-R	5′-CGTCCTTGAAGAAATGCAGA-3′
Rat-*MMP13*-F	5′-CAAGCAGCTCCAAAGGCTAC-3′
Rat-*MMP13*-R	5′-TGGCTTTTGCCAGTGTAGGT-3′
Rat-*COX-2*-F	5′-CTCAGCCATGCAGCAAATCC-3′
Rat-*COX-2*-R	5′-GGGTGGGCTTCAGCAGTAAT-3′
Rat-*IL-1β*-F	5′-CAGCTTTCGACAGTGAGGAGA-3′
Rat-*IL-1β*-R	5′-TTGTCGAGATGCTGCTGTGA-3′
Rat-*IL-6*-F	5′-TCTCCGCAAGAGACTTCCAG-3′
Rat-*IL-6*-R	5′-AGCCTCCGACTTGTGAAGTG-3′
Rat-*α-SMA*-F	5′-GCTGGTGATGATGCTCCCAG-3′
Rat-*a-SMA*-R	5′-TCAGGGTCAGGATCCCTCTC-3′
Rat-*GAPDH*-F	5′-GGTGAAGGTCGGTGTGAACG-3′
Rat-*GAPDH*-R	5′-CTCGCTCCTGGAAGATGGTG-3′
F: Forward; R: Reverse	

Table 3
Primary antibodies for IF cell staining.

Primary Antibody	Catalog Number	Dilution Ratio	Source
Acan	13880-1-AP	1:100	Proteintech Group, Wuhan, Hubei, China
MMP13	18165-1-AP	1:50	Proteintech Group, Wuhan, Hubei, China
Col1a1	# 84,336	1:200	Cell Signaling Technology, Beverly, MA, USA
α-SMA	#19245	1:200	Cell Signaling Technology, Beverly, MA, USA
p-P65	#3033	1:200	Cell Signaling Technology, Beverly, MA, USA

experiments. Hematoxylin-eosin (Servicebio, China) and safranin O/fast green staining (Servicebio, China) were performed according to the manufacturer's protocols. The primary antibodies used in IHC assays are listed in Table 4. All bright-field images were captured using a microscope (EVOS fl auto, Thermo Fisher Scientific, USA) and analyzed using ImageJ software.

2.9. Animal model generation and treatment

For *in vivo* experiments, thirty-six rat IVDD model establishment and IVD local injection had been detailed according our previous study [31]. In this study, different intervention methods were used for consecutive IVDs in rat coccygeal (Co; Co6/7 – Co9/10) of the same individual to reduce errors caused by individual differences. The NP tissues in Co6/7 –

2.8. Immunohistochemistry (IHC) and staining assay

Freshly dissected spinal tissues were fixed with 4% PFA, decalcificated, embedded in paraffin wax, and transferred to a slice for further

Table 4
Primary antibodies for IHC staining.

Primary Antibody	Catalog Number	Dilution Ratio	Source
Col1a1	# 84,336	1:100	Cell Signaling Technology, Beverly, MA, USA
Acan	13880-1-AP	1:200	Proteintech Group, Wuhan, Hubei, China
MMP13	18165-1-AP	1:100	Proteintech Group, Wuhan, Hubei, China
MMP9	10375-2-AP	1:100	Proteintech Group, Wuhan, Hubei, China

Co9/10 of each rats were divided into four groups as follows: (1) The SHAM group received sham operation and injected with 2 μl vehicle in the NP tissues of Co6/7. (2) The SHAM + PA group received sham operation and injected with 2 μl 20 μM PA in the NP tissues of Co7/8. (3) The IVDD group was punctured and injected 2 μl vehicle in the NP tissues of Co8/9. (4) The IVDD + PA group was punctured and injected with 2 μl 20 μM PA in the NP tissues of Co9/10. X-ray, micro-CT, MRI, and IHC of the model IVD were performed at 2, 4, 6, and 8 weeks after surgery.

2.10. Magnetic resonance imaging (MRI)

MRI was performed using a UNITED IMAGING 3.0-TMR scanner (Shanghai, China). During imaging, the rats were anesthetized with a 2% isoflurane/oxygen mixture and placed in the prone position with the tail straight. Twenty consecutive sagittal and coronal T2-weighted images were obtained via scanning the surgical region of the rats with a double-tuned-volume radiofrequency coil. Finally, the MRI images were analyzed using the Pfirrmann score [32].

2.11. Micro-CT

After anesthesia and positioning as mentioned above, rat's disc micro-CT scanning was performed using microcomputed tomography (Scanco Medical, Switzerland). The CT scanning parameters were set as follows: voltage = 100 kV, current = 98 μA, and voxel size = 10 μm. Three-dimensional CT (CT-3D) images and X-ray images were obtained from the evaluation system built-in the microcomputed tomography system.

2.12. Statistical analysis

One-way analysis of variance was performed to analyze data between multiple experimental group comparisons, whereas the Kruskal–Wallis H test was chosen to analyze ordinal variable comparisons, such as histological staining score and Pfirrmann score (data are presented as medians with interquartile ranges). All statistical graph generation and analysis of related-data were performed using GraphPad Prism 8 and presented as mean ± standard deviation (SD). Statistical significance was considered as $*p < 0.05$, $**p < 0.01$, $***p < 0.001$.

3. Results

3.1. Cytotoxicity of PA, IL-1β, and TGF-β1 on NP cell

We first performed cytotoxicity assays for the reagents used in the *in vitro* experiments. After different concentrations (0–20 ng/ml) or different durations (0–48 h) of IL-1β stimulation, NP cells showed no apparent cytotoxicity (Fig. 1A and B). Similarly, PA (20 μM) and TGF-β1 (10 ng/ml) administered at experimental concentrations either alone or in combination for 48 h showed no evident side effects on cell viability (Fig. 1C and D).

3.2. Effect of IL-1β on the ECM metabolism of NP cells

To mimic the inflammatory degeneration cell model, IL-1β, a key pro-inflammatory cytokine, is often used to induce inflammatory and degenerative NP cells. Among different IL-1β concentration or duration treatments (Fig. 1E–H), ECM metabolism phenotypes changed significantly after treatment with 5 ng/ml IL-1β for 48 h. Under these inflammatory conditions, anabolic protein levels (Acan and Col2a1) were significantly down–regulated, whereas those of catabolic (MMP3 and MMP13) and inflammatory marker (iNOS) were up–regulated, which represents the inflammatory degeneration process of NP cells. Therefore, 5 ng/ml of IL-1β was applied to stimulate NP cells for 48 h in the subsequent experiments.

3.3. PA improves inflammation and reverses degenerative phenotypes in NP cells

To investigate the effect of PA on ECM metabolism and the inflammatory environment during IVDD progression, the differences in the expression of major ECM synthesis and degrading genes and secreted inflammatory factors were investigated via inflammatory factor (IL-1β) and PA treatment. At the protein level, the expression of MMP3, MMP9, and MMP13 and inflammatory factors, such as IL-1β, IL-6 and COX-2, increased significantly after IL-1β exposure, whereas Acan and Col2a1 levels were downregulated. However, these degenerative and inflammatory phenotypes were reversed when the NP cells were treated with 20 μM PA (Fig. 2A and B). Similar trends were detected in mRNA expression under the same intervention conditions (Fig. 2G). The IF images showed decreased Acan expression and increased MMP13 expression after IL-1β stimulation, and PA treatment attenuated this ECM degeneration (Fig. 2C–F). Therefore, PA has the potential to improve NP cell degeneration and metabolic function and alleviate inflammation. Moreover, TGF-β1 and Col1a1 were associated with the process of NP fibrosis, and their elevated expression level was also regulated by IL-1β and inhibited by PA (Fig. 2A and B).

3.4. PA reduces inflammation by inhibiting the NF-κB and MAPK signaling pathways

The NF-κB and MAPK signaling pathways play crucial roles in cellular activities, including maintaining various physiological activities of cells and transmitting signals. The activation of the MAPK and NF-κB signaling pathways triggers an inflammatory response and promotes NP degeneration, whereas inhibition of these pathways contributes to alleviation of IVDD progression [33]. In NP cells, the NF-κB (p-P65) and MAPK pathways (p-P38, p-JNK, p-ERK) were significantly activated 15 min after IL-1β stimulation and gradually weakened (Fig. 3A and B). Thus, we subsequently administered PA 15 min after IL-1β intervention to explore the effect of PA on these inflammatory pathways. As shown in Fig. 3C and D, p-IKKα/β was activated, leading to IκBα depolymerization and phosphorylation, as well as subsequent P65 phosphorylation, after IL-1β treatment. Moreover, p-P65, which is an activated nuclear factor, was preferentially distributed in the nucleus rather than the cytoplasm after inflammatory irritation (Fig. 3E and F). This series of NF-κB-related inflammatory pathway activation processes can be inhibited by PA treatment (Fig. 3C–F). The MAPK pathway showed similar inflammatory factor-induced activation and PA blockade effects (Fig. 3G and H). These results suggest that PA can reduce inflammation by blocking the NF-κB and MAPK signaling pathways.

3.5. PA enhanced the autophagy process via blocking the PI3K/AKT/ mTOR signaling pathway

Autophagy is a host defense mechanism in mammalian cells that is not only closely related to cell metabolism, proliferation, and apoptosis, but also participates in the pathological process of various degenerative
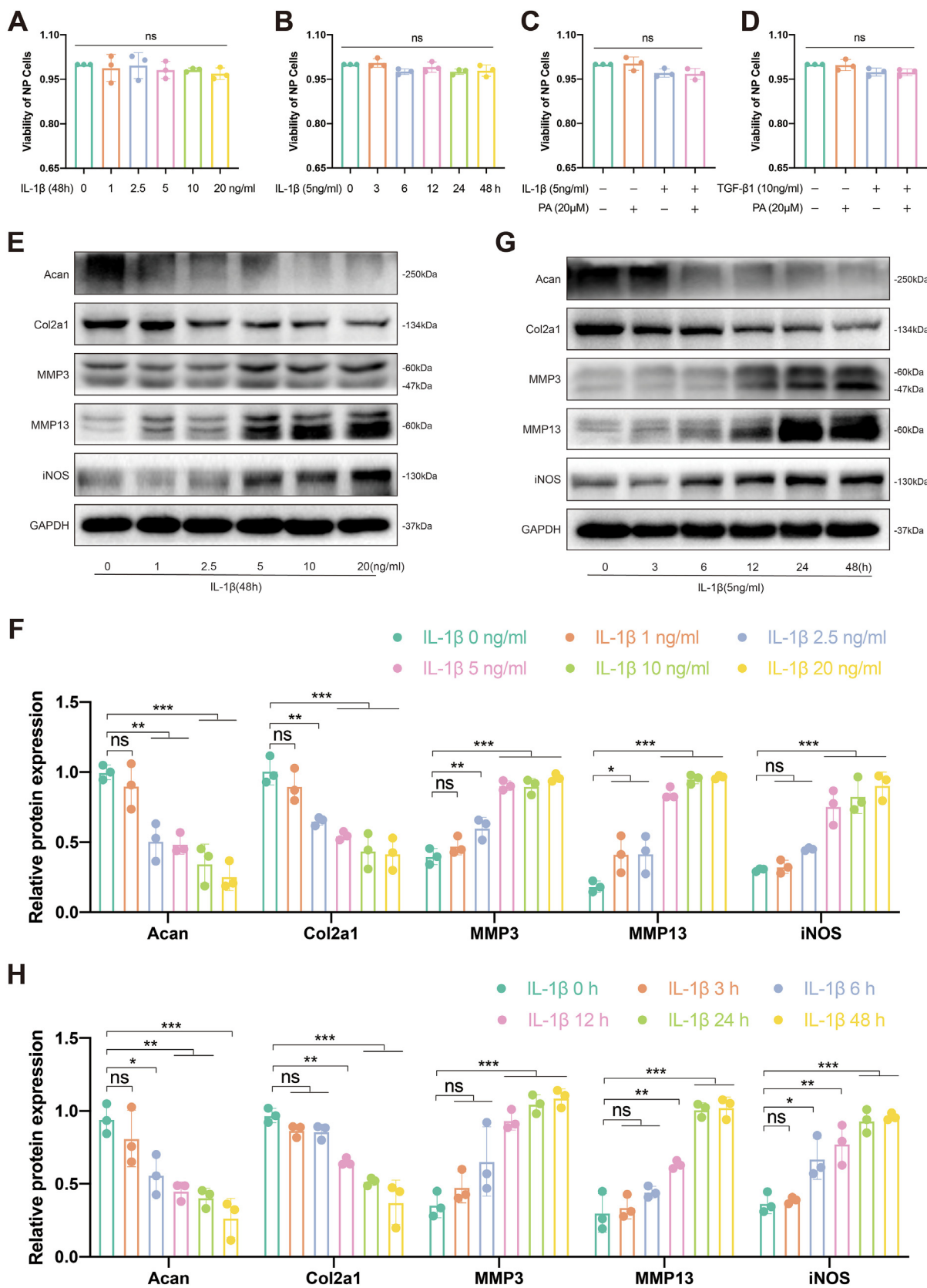
Figure 1. IL-1β promotes ECM degeneration (A–D) Cell viability assay for reagents (PA, IL-1β, and TGF-β1) was performed **(E)** The representative western blot of ECM components after receiving different concentrations (0, 1, 2.5, 5, 10, and 20 ng/ml) of IL-1β stimulation for 48 h, and **(F)** its quantification **(G)** The representative western blot of ECM components after receiving 5 ng/ml of IL-1β stimulation for different durations (0, 3, 6, 12, 24, and 48 h), and **(H)** its quantification.
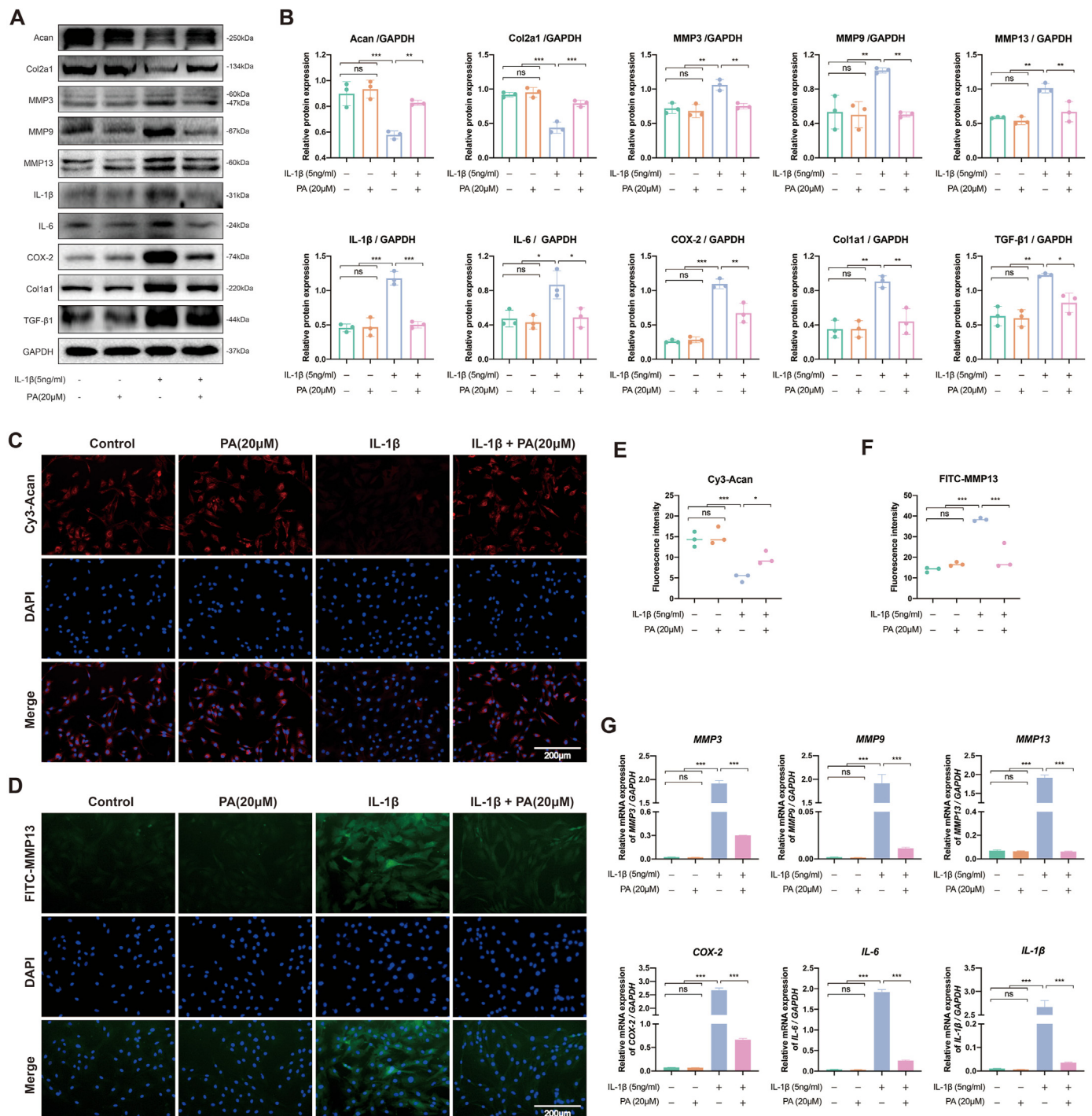
Figure 2. PA improves ECM degeneration and inflammation (A) The representative western blot of ECM components, inflammation and fibrosis markers, and **(B)** their quantification after receiving 5 ng/ml IL-1β and 20 μM PA alone or in combination for 48 h. The IF images of **(C)** Acan and **(D)** MMP13, and their **(E, F)** fluorescence intensity quantification **(G)** mRNA level of ECM degrading genes and inflammatory factors determined using RT-qPCR.

diseases [34,35]. However, proper activation of autophagy can prevent apoptosis and aging and may play a protective role in degenerative diseases [36]. The PI3K/AKT/mTOR signaling pathway regulates autophagy, and its inhibition enhances enhanced autophagy [37]. The PI3K/AKT/mTOR signaling pathway was activated after short-term stimulation with IL-1β in NP cells (Fig. 4A and B) and inhibited by PA (Fig. 4C and D). Furthermore, as shown in Fig. 4E and F, PA rescued the autophagy process that was impaired by inflammation which decreased Atg3, Atg7, LC3 I/II, Beclin-1, and increased P62. These results suggest

that PA may enhance autophagy in degenerated NP cells by blocking the PI3K/AKT/mTOR pathway.

3.6. PA inhibits TGF-β1-induced fibrosis in NP cells

TGF-β1 is an important factor that drives tissue fibrosis and can directly activate SMAD signal transduction, thereby triggering the overexpression of fibrotic proteins. As mentioned above (Fig. 2A and B), NP cells increased TGF-β1 secretion and induced fibrosis under IL-1β
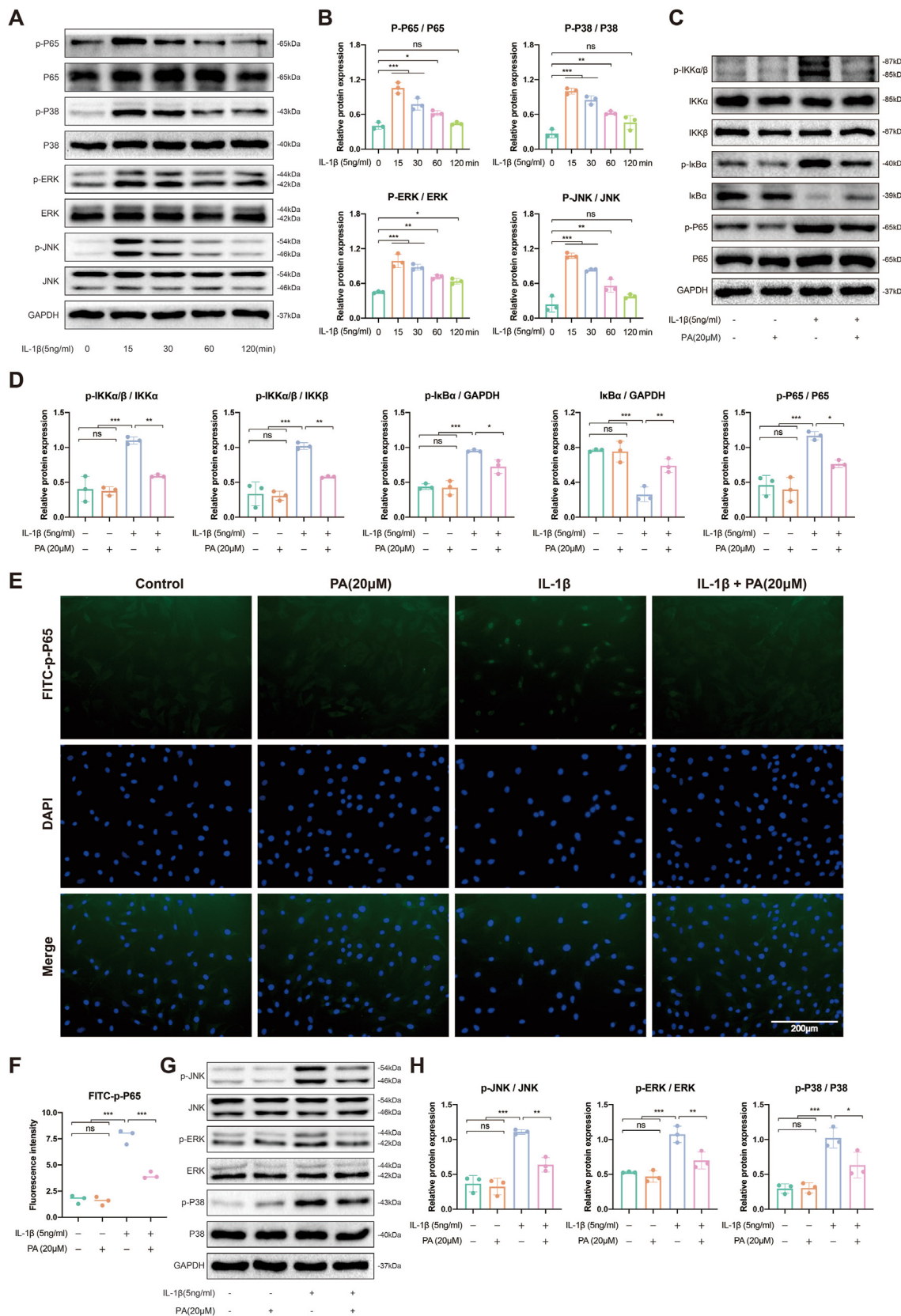
Figure 3. PA inhibits NF-κB and MAPK signaling pathways (A) The representative western blot of NF-κB and MAPK pathway proteins after receiving 5 ng/ml IL-1β stimulation for different durations (0, 15, 30, 60, and 120 min), and **(B)** its quantification **(C)** The representative western blot of NF-κB pathway proteins after receiving 5 ng/ml IL-1β for 15 min and 20 μM PA alon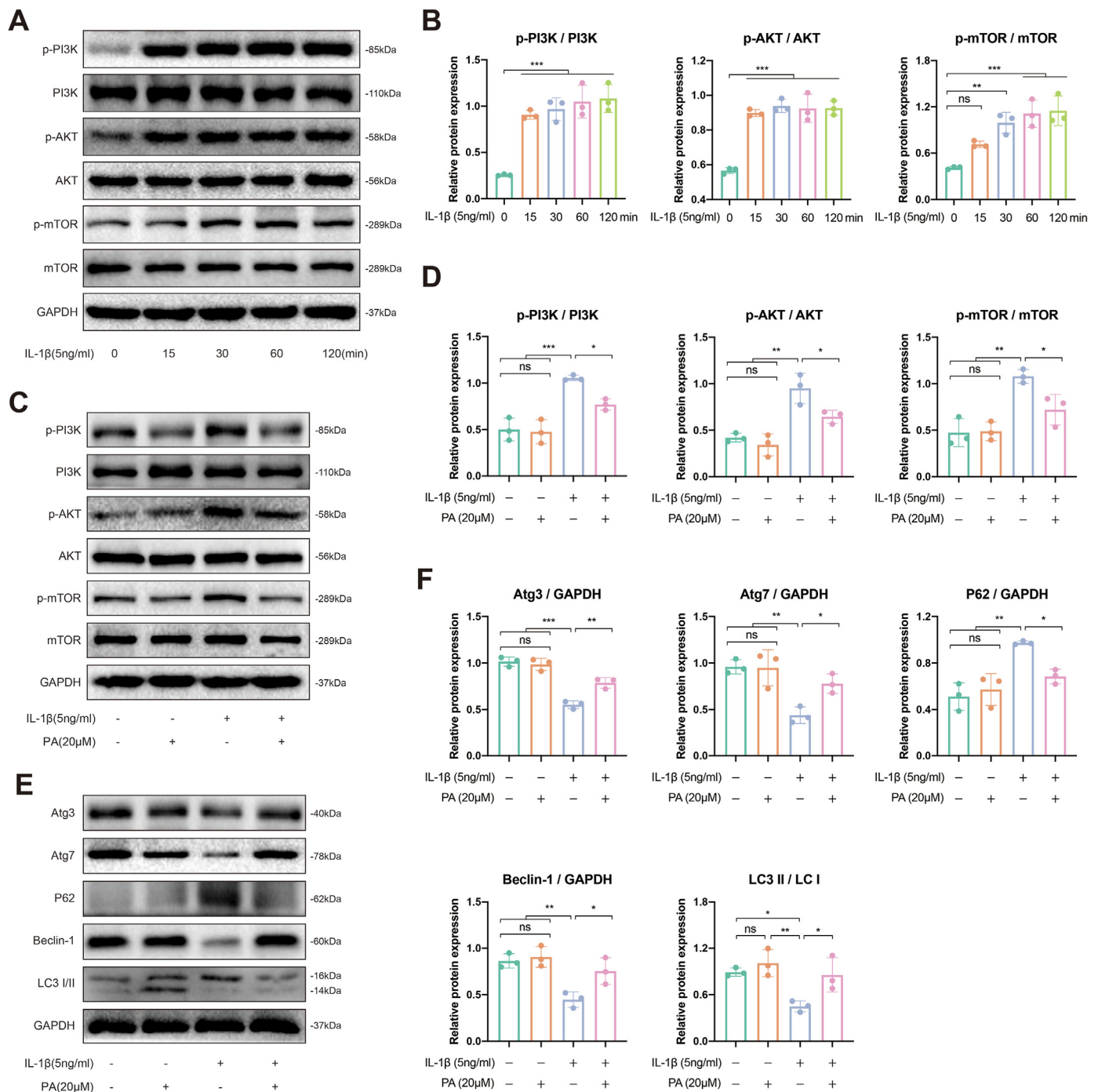e or in combination for 48 h, and **(D)** its quantification **(E)** IF analysis of p-P65 and its **(F)** fluorescence intensity quantification **(G)** The representative western blot of MAPK pathway proteins after receiving 5 ng/ml IL-1β for 15 min and 20 μM PA alone or in combination for 48 h, and **(H)** its quantification.

Figure 4. PA enhances autophagy by inhibiting the PI3K/AKT/mTOR pathway (A) The representative western blot of PI3K/AKT/mTOR pathway proteins after receiving 5 ng/ml IL-1β stimulation for different durations (0, 15, 30, 60, and 120 min), and **(B)** its quantification. After receiving 5 ng/ml IL-1β for 1 h and 20 μM PA alone or in combination for 48 h, the representative western blot of **(C)** PI3K/AKT/mTOR pathway proteins and **(E)** autophagy-related proteins, and **(D, F)** its quantification, respectively.

prolonged stimulation (48 h; Fig. 5A–D). Subsequently, 10 ng/ml TGF-β1 was used to stimulate NP cells to establish a cellular model of fibrosis. TGF-β1 not only activated SMAD2/3 phosphorylation, but also upregulated fibrotic proteins (Col1a1 and α-SMA) and promoted NP matrix degeneration (Acan and Col2a1) (Fig. 5E–H). Moreover, PA treatment alleviated this fibrotic process and ECM degeneration. Similar trends were also confirmed by the IF images; upregulated fibrotic protein levels were inhibited by PA administration (Fig. 5I–L). The anti-fibrotic effect of PA was verified via RT-qPCR (Fig. 5M). Additionally, inflammation accelerates NP cell fibrosis, which, in turn, further induces the secretion of

inflammatory cytokines (IL-1β and IL-6). Therefore, inflammation and fibrosis interact during IVDD progression, and PA has the potential to disrupt this vicious cycle.

3.7. PA alleviates disc degradation in rat IVDD model

To investigate the therapeutic efficacy of PA *in vivo*, a rat IVDD model continuous disc was induced. At 2, 4, 6, and 8 weeks after the operation, X-ray, micro-CT, and MRI were performed on the surgical area of the caudal vertebra in the rat model. The IVDD disc images revealed
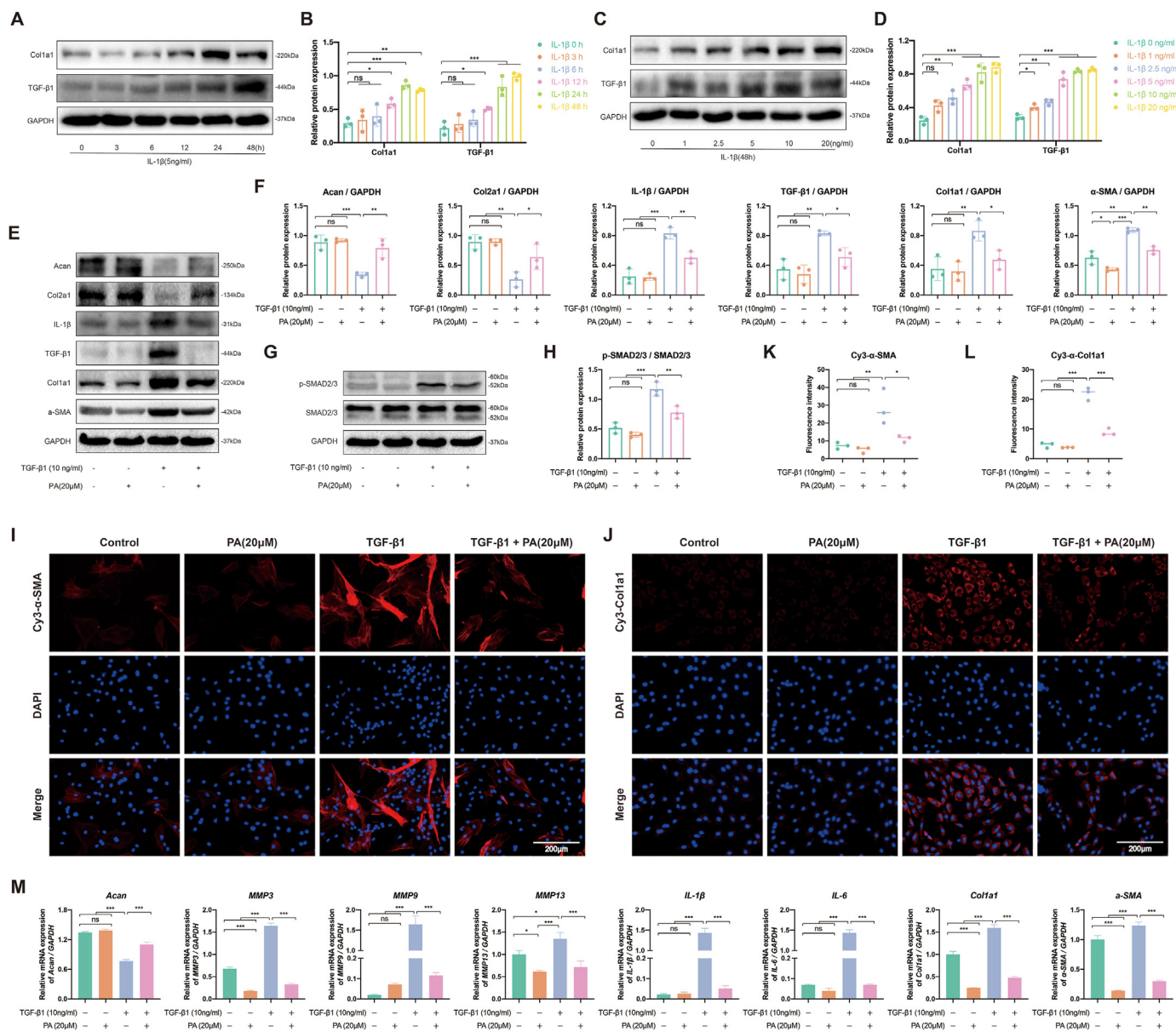
Figure 5. PA inhibits NP cell fibrosis by inhibiting the SMAD2/3 pathway. The representative western blot of fibrosis marker after receiving **(A)** different concentrations (0, 1, 2.5, 5, 10, and 20 ng/ml) or **(C)** different durations (0, 3, 6, 12, 24, and 48 h) of IL-1β stimulation, and **(B, D)** its quantification, respectively. After receiving 10 ng/ml TGF-β1 and 20 μM PA alone or in combination for 48 h, the representative western blot of **(E)** ECM components, inflammation and fibrosis markers **(G)** SMAD2/3 pathway proteins, and **(F, H)** its quantification, respectively. IF analysis of **(I)** α-SMA and **(J)** Col1a1, and its **(K, L)** fluorescence intensity quantification, respectively **(M)** mRNA level of ECM components, inflammation, and fibrosis markers gene determined using RT-qPCR.

degenerative changes, intervertebral space stenosis, and altered structures of the coccygeal intervertebral discs after surgery, whereas the disc treated with PA regressed to a noticeable improvement (Fig. 6). Moreover, H&E staining and Safranin O/Fast Green staining of the rat IVDD model showed ECM reduction and fibrosis aggravation after acupuncture compared to the discs concurrently receiving PA therapy (Fig. 7A–C). Additionally, MMP9, MMP13, and Col1a1 expressions were significantly upregulated, and Acan synthesis was reduced in IVDD-disc, whereas degenerative discs that received PA treatment suppressed this deterioration trend (Fig. 7D and E). These *in vivo* results suggest that PA treatment was beneficial in reducing inflammation and fibrosis, thus, improving IVDD progression.

4. Discussion

IVDD progression can cause a series of chronic and progressive pain and neurological symptoms, thus, reducing the patient's ability to perform daily activities [38]. At present, although various traditional therapies are being used in partial IVDD cases, patients still do not to benefit from long-term treatment, as it is attributed to the risk of recurrent attacks, surgery, and drug side effects [39,40]. To treat IVDD fundamentally, rather than to relieve symptoms, treatments focusing on IVDD-related pathogenesis are the emerging trends in the field. Pathogenic mechanisms, such as inflammation, autophagy, and fibrosis, may act as potential therapeutic targets for IVDD [24,41]. As an effective
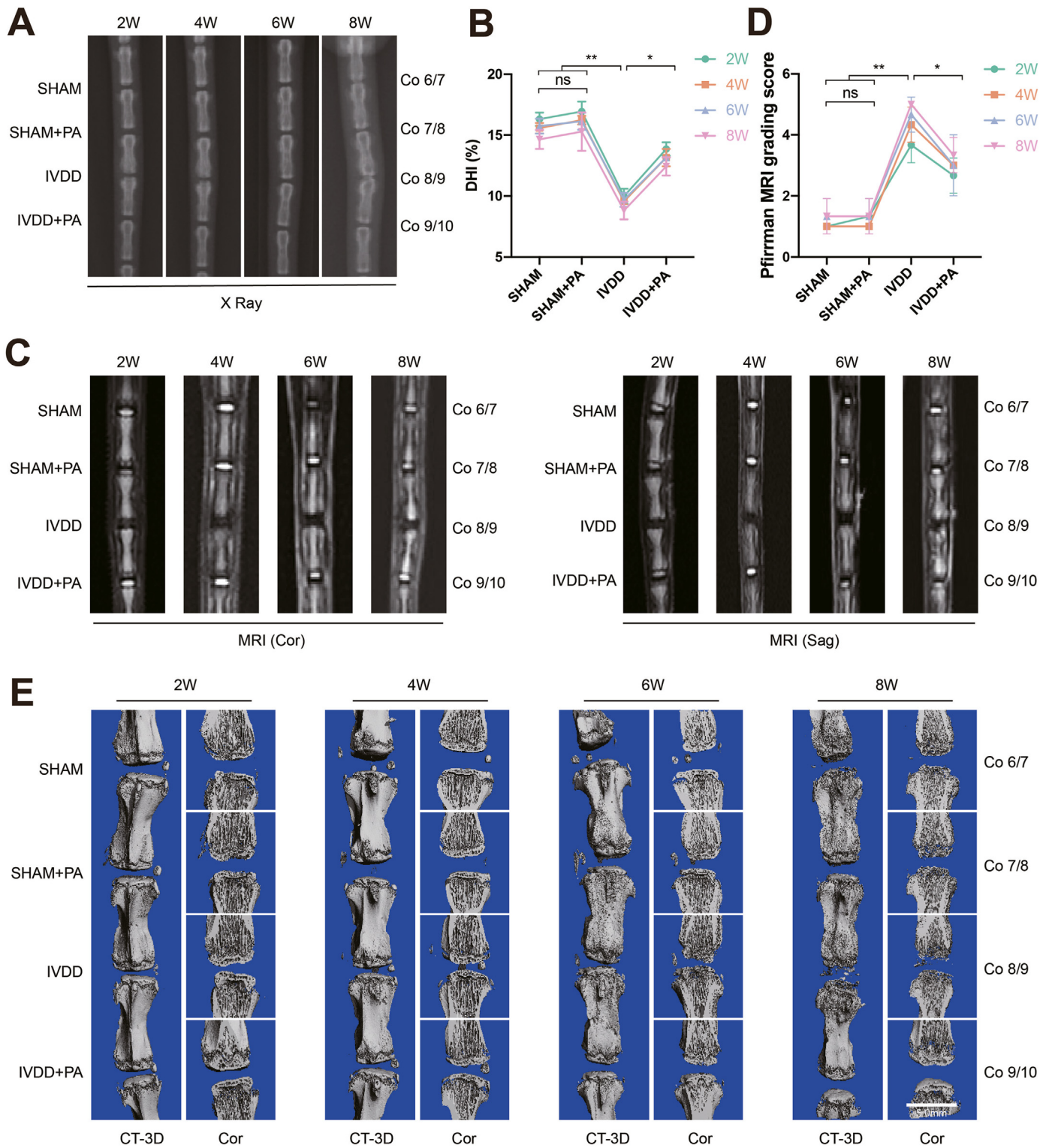
Figure 6. Imaging analysis of PA effects in rat IVDD model (A) The representative X-ray images of rat models, and **(B)** its DHI measurement **(C)** The representative MRI images of rat models, and **(D)** its Pfirrmann score evaluation **(E)** The representative Mirco-CT images of rat models.

strategy to prevent and treat IVDD pathogenesis, this study is the first to report that PA not only reduces inflammation and fibrosis, but also promotes autophagy, thereby improving IVDD progression.

IVDD pathogenesis can be attributed to various mechanisms, such as inflammation [42], apoptosis [43], autophagy [44,45], fibrosis [46,47], and metabolic disorders [40,48,49]. The inflammatory landscape is composed of the activation of multiple inflammatory pathways and the secretion of multiple inflammatory factors as the main facilitator to accelerate IVDD progression [50]. Based on extensive research, NF-κB and MAPK pathways are crucial inflammatory pathways involved in progression of degeneration diseases, such as IVDD and osteoarthritis, and its activation may lead to secretion of inflammatory cytokines and dysfunction of ECM synthesis [51–53]. In this study, IL-1β was used to stimulate NP cells to mimic inflammatory and degenerative disc
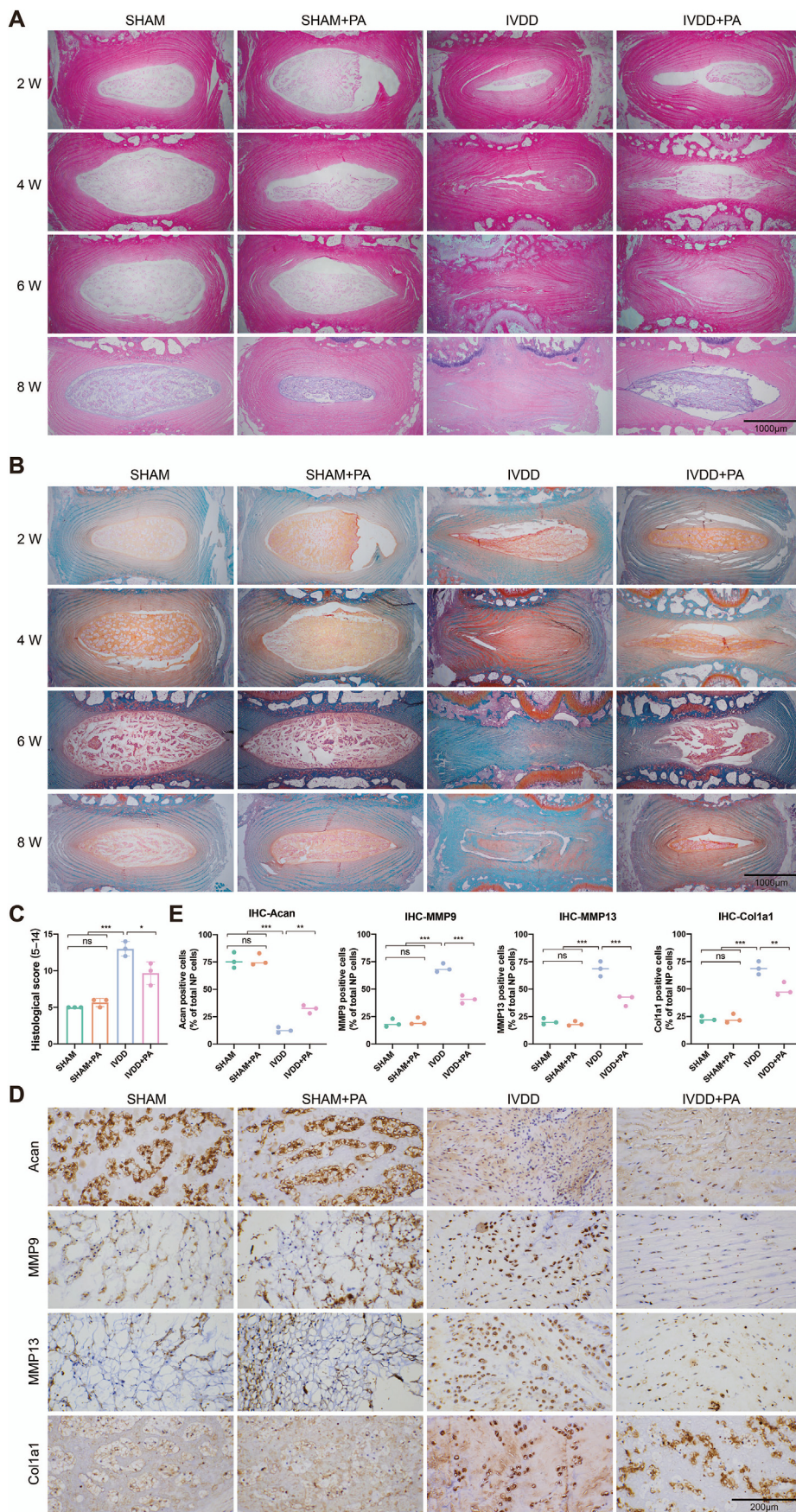
Figure 7. Effects of PA in rat IVDD model (A) H&E staining and **(B)** Safranin O/Fast Green staining of rat IVDD model, and **(C)** its histological score evaluation **(D)** IHC images of Acan, MMP13, MMP9, Col1a1, and **(E)** its positive cell quantification.
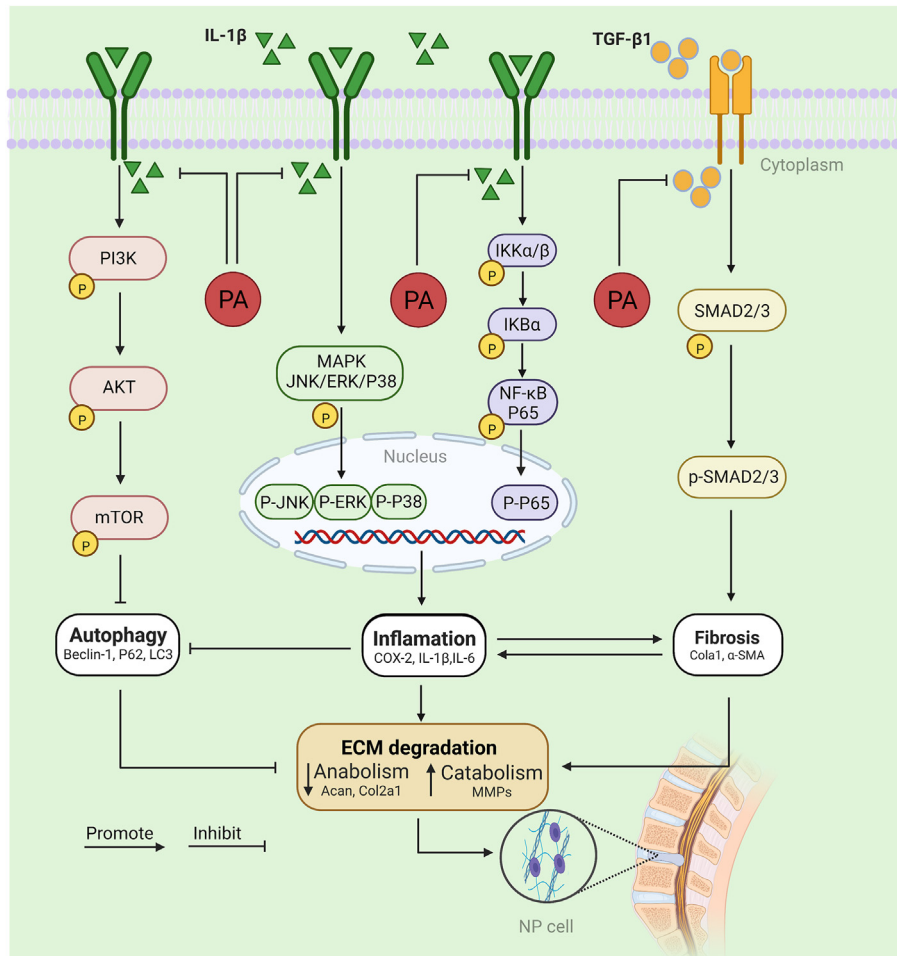
Figure 8. Schematic illustration of the mechanism by which PA alleviates IVDD progression (figure was created with BioRender.com).

environments *in vitro*. Although inflammatory stimulation enables the rapid activation of inflammatory pathways (NF-κB and MAPK pathways) and subsequent degeneration of NP cells [54,55], PA treatment can improve these adverse effects and cell degeneration. Moreover, IL-1β is a risk factor for cellular homeostasis disruption, leading to autophagy disorders [56]. Our results showed that PA treatment could recover the autophagy of NP cells, which interferes with IL-1β, by blocking the PI3K/AKT/mTOR pathway. Thus, PA exerted a protective effect in restoring IVD tissues against IL-1β irritation.

Fibrosis of NP tissues is one of the late pathological changes in IVDD progression that may lead to increased hardness, elasticity loss, or nerve compression [57]. TGF-β1 is closely associated with the fibrotic process and mechanisms of various diseases [58–60]. Although TGF-β1 may contribute to IVD development and growth, excessive TGF-β signaling activation exacerbates IVDD through promoting fibrotic progression, cell senescence, and apoptosis [61]. Our experimental results showed that NP cells had significantly increased TGF-β1 secretion after IL-1β stimulation, consistent with the Wataru Morita result tendency in the torn tendon study [62]. After TGF-β1 treatment, the SMAD2/3 pathway is activated and phosphorylated, which upregulates the expression levels of downstream fibrotic proteins (α-SMA and Col1a1) and inflammatory mediators (IL-1β and IL-6), thereby leading to IVD fibrosis and worsening of inflammation. Recent research reported that the overexpression of TGF-β1 could aggravate the upregulation of detrimental factors, such as IL-6, TNF-α, collagen I, and collagen III in NP cells, this also confirms our research results [63]. Therefore, fibrosis and inflammation of the IVD forms a vicious cycle that results in persistent IVDD aggravation. PA treatment also effectively improved IVD fibrosis by inhibiting the

SMAD2/3 pathway and can, therefore, be expected to break this vicious cycle.

Furthermore, PA application to acupuncture discs can effectively alleviate IVDD progression in rat models. Although PA has shown excellent anti-inflammatory, anti-fibrotic, and autophagy-promoting effects in *vivo* and *in vitro* experiments, further clinical applications still has some limitations to. First, the direct and noninvasive intervention in the IVD is difficult, and drug delivery systems targeting the IVD remain unexplored. Second, we only revealed the effect of PA on IVDD-related classical signaling pathways in this study, whereas its effects on other targets or diseases remain to be explored. Despite these limitations, our research undeniably provides the possibility of a potential theoretical basis for PA applications against IVDD.

5. Conclusion

In summary, through a series of *in vivo* and *in vitro* experiments, we found that PA treatment exhibited significant anti-inflammatory, anti-fibrotic, and autophagic effects during IVDD progression. Further investigation of these effects revealed that PA not only regulated the NF-κB and MAPK pathways, leading to reduced inflammation, but also improved autophagy by blocking the PI3K/AKT/mTOR pathway. Additionally, PA exerted anti-fibrotic effects by downregulating the SMAD2/3 pathway and its downstream proteins (Fig. 8). In animal experiments, PA showed an anti-degenerative effect in a rat IVDD model with no additional side effects. These encouraging results suggest that PA may be an effective and potential drug for clinical treatment of IVDD pathogenesis.

Credit author contribution statement

Funding sources

Ethics statement

The study were conducted following the guidelines of the International Guiding Principles for Animal Research and approved by the Ethics Committee of Huazhong University of Science and Technology.

Data availability statement

The data supporting the findings are presented in the article/supplementary materials, further inquiries can be directed to the corresponding author.

Declaration of competing interest

The authors declare that they have no known competing financial interests or personal relationships that could have appeared to influence the work reported in this paper.

References

[1] Williams RJ, Tryfonidou MA, Snuggs JW, Le Maitre CL. Cell sources for nucleus pulposus regeneration. JOR Spine 2021;4(4):e1175. https://doi.org/10.1002/jsp2.1175.

[2] Sun Z, Liu ZH, Chen YF, Zhang YZ, Wan ZY, Zhang WL, et al. Molecular immunotherapy might shed a light on the treatment strategies for disc degeneration and herniation. Med Hypotheses 2013;81(3):477–80. https://doi.org/10.1016/j.mehy.2013.06.014.

[3] Wang F, Cai F, Shi R, Wang XH, Wu XT. Aging and age related stresses: a senescence mechanism of intervertebral disc degeneration. Osteoarthritis Cartilage 2016;24(3):398–408. https://doi.org/10.1016/j.joca.2015.09.019.

[4] Chen J, Xuan J, Gu YT, Shi KS, Xie JJ, Chen JX, et al. Celastrol reduces IL-1β induced matrix catabolism, oxidative stress and inflammation in human nucleus pulposus cells and attenuates rat intervertebral disc degeneration in vivo. Biomed Pharmacother 2017;91:208–19. https://doi.org/10.1016/j.biopha.2017.04.093.

[5] Risbud MV, Shapiro IM. Role of cytokines in intervertebral disc degeneration: pain and disc content. Nat Rev Rheumatol 2014;10(1):44–56. https://doi.org/10.1038/nrrheum.2013.160.

[6] Manav V, İlhan D, Mercan H, Kılıç A, Polat AK, Aksu AEK. Association between intervertebral disc degeneration and Behçet's disease. Dermatol Ther 2022;35(7):e15585. https://doi.org/10.1111/dth.15585.

[7] Capossela S, Schläfli P, Bertolo A, Janner T, Stadler BM, Pötzel T, et al. Degenerated human intervertebral discs contain autoantibodies against extracellular matrix proteins. Eur Cell Mater 2014;27:251–63. ; discussion 263.10.22203/ecm.v027a18.

[8] Luo L, Jian X, Sun H, Qin J, Wang Y, Zhang J, et al. Cartilage endplate stem cells inhibit intervertebral disc degeneration by releasing exosomes to nucleus pulposus cells to activate Akt/autophagy. Stem Cells 2021;39(4):467–81. https://doi.org/10.1002/stem.3322.

[9] Calvo-Echenique A, Cegoñino J, Correa-Martín L, Bances L, Palomar AP. Intervertebral disc degeneration: an experimental and numerical study using a rabbit model. Med Biol Eng Comput 2018;56(5):865–77. https://doi.org/10.1007/s11517-017-1738-3.

[10] Menon RG, Zibetti MVW, Pendola M, Regatte RR. Measurement of Three-Dimensional Internal Dynamic Strains in the Intervertebral Disc of the Lumbar Spine With Mechanical Loading and Golden-Angle Radial Sparse Parallel-Magnetic Resonance Imaging. J Magn Reson Imaging 2021;54(2):486–96. https://doi.org/10.1002/jmri.27591.

[11] Wang WJ, Yu XH, Wang C, Yang W, He WS, Zhang SJ, et al. MMPs and ADAMTSs in intervertebral disc degeneration. Clin Chim Acta 2015;448:238–46. https://doi.org/10.1016/j.cca.2015.06.023.

[12] Yang W, Yu XH, Wang C, He WS, Zhang SJ, Yan YG, et al. Interleukin-1β in intervertebral disk degeneration. Clin Chim Acta 2015;450:262–72. https://doi.org/10.1016/j.cca.2015.08.029.

[13] Hanaei S, Abdollahzade S, Khoshnevisan A, Kepler CK, Rezaei N. Genetic aspects of intervertebral disc degeneration. Rev Neurosci 2015;26(5):581–606. https://doi.org/10.1515/revneuro-2014-0077.

[14] Yang F, Liu W, Huang Y, Yang S, Shao Z, Cai X, et al. Regulated cell death: Implications for intervertebral disc degeneration and therapy. J Orthop Translat 2022;37:163–72. https://doi.org/10.1016/j.jot.2022.10.009.

[15] Zhao K, An R, Xiang Q, Li G, Wang K, Song Y, et al. Acid-sensing ion channels regulate nucleus pulposus cell inflammation and pyroptosis via the NLRP3 inflammasome in intervertebral disc degeneration. Cell Prolif 2021;54(1):e12941. https://doi.org/10.1111/cpr.12941.

[16] Kang L, Zhang H, Jia C, Zhang R, Shen C. Targeting Oxidative Stress and Inflammation in Intervertebral Disc Degeneration: Therapeutic Perspectives of Phytochemicals. Front Pharmacol 2022;13:956355. https://doi.org/10.3389/fphar.2022.956355.

[17] Wang X, Chen S, Zhao Z, Chen F, Huang Y, Guo X, et al. Genomic G-quadruplex folding triggers a cytokine-mediated inflammatory feedback loop to aggravate inflammatory diseases. iScience 2022;25(11):105312. https://doi.org/10.1016/j.isci.2022.105312.

[18] Yi W, Wen Y, Tan F, Liu X, Lan H, Ye H, et al. Impact of NF-κB pathway on the apoptosis-inflammation-autophagy crosstalk in human degenerative nucleus pulposus cells. Aging (Albany NY) 2019;11(17):7294–306. https://doi.org/10.18632/aging.102266.

[19] Mack M. Inflammation and fibrosis. Matrix Biol 2018;68-69:106–21. https://doi.org/10.1016/j.matbio.2017.11.010.

[20] Wang Y, Che M, Xin J, Zheng Z, Li J, Zhang S. The role of IL-1β and TNF-α in intervertebral disc degeneration. Biomed Pharmacother 2020;131:110660. https://doi.org/10.1016/j.biopha.2020.110660.

[21] Zhang WJ, Chen SJ, Zhou SC, Wu SZ, Wang H. Inflammasomes and Fibrosis. Front Immunol 2021;12:643149. https://doi.org/10.3389/fimmu.2021.643149.

[22] Castro AL, Ribeiro-Machado C, Oliveira CM, Teixeira GQ, Neidlinger-Wilke C, Pereira P, et al. Fibrotic alterations in human annulus fibrosus correlate with progression of intervertebral disc herniation. Arthritis Res Ther 2022;24(1):25. https://doi.org/10.1186/s13075-021-02690-w.

[23] Xia C, Zeng Z, Fang B, Tao M, Gu C, Zheng L, et al. Mesenchymal stem cell-derived exosomes ameliorate intervertebral disc degeneration via anti-oxidant and anti-inflammatory effects. Free Radic Biol Med 2019;143:1–15. https://doi.org/10.1016/j.freeradbiomed.2019.07.026.

[24] Sun Y, Lyu M, Lu Q, Cheung K, Leung V. Current Perspectives on Nucleus Pulposus Fibrosis in Disc Degeneration and Repair. Int J Mol Sci 2022;23(12). https://doi.org/10.3390/ijms23126612.

[25] Wang L, Gu J, Zong M, Zhang Q, Li H, Li D, et al. Anti-inflammatory action of physalin A by blocking the activation of NF-κB signaling pathway. J Ethnopharmacol 2021;267:113490. https://doi.org/10.1016/j.jep.2020.113490.

[26] Lu R, Yu X, Liang S, Cheng P, Wang Z, He ZY, et al. Physalin A Inhibits MAPK and NF-κB Signal Transduction Through Integrin αVβ3 and Exerts Chondroprotective Effect. Front Pharmacol 2021;12:761922. https://doi.org/10.3389/fphar.2021.761922.

[27] Lin YH, Hsiao YH, Ng KL, Kuo YH, Lim YP, Hsieh WT. Physalin A attenuates inflammation through down-regulating c-Jun NH2 kinase phosphorylation/Activator Protein 1 activation and up-regulating the antioxidant activity. Toxicol Appl Pharmacol 2020;402:115115. https://doi.org/10.1016/j.taap.2020.115115.

[28] He H, Zang LH, Feng YS, Wang J, Liu WW, Chen LX, et al. Physalin A induces apoptotic cell death and protective autophagy in HT1080 human fibrosarcoma cells. J Nat Prod 2013;76(5):880–8. https://doi.org/10.1021/np400017k.

[29] Kang N, Jian JF, Cao SJ, Zhang Q, Mao YW, Huang YY, et al. Physalin A induces G2/M phase cell cycle arrest in human non-small cell lung cancer cells: involvement of the p38 MAPK/ROS pathway. Mol Cell Biochem 2016;415(1-2):145–55. https://doi.org/10.1007/s11010-016-2686-1.

[30] Xiang D, Zou J, Zhu X, Chen X, Luo J, Kong L, et al. Physalin D attenuates hepatic stellate cell activation and liver fibrosis by blocking TGF-β/Smad and YAP signaling. Phytomedicine 2020;78:153294. https://doi.org/10.1016/j.phymed.2020.153294.

[31] Xu H, Wei K, Tu J, Chen Y, He Y, Ding Y, et al. Reducing Inflammation and Vascular Invasion in Intervertebral Disc Degeneration via Cystathionine-γ-Lyase Inhibitory Effect on E-Selectin. Front Cell Dev Biol 2021;9:741046. https://doi.org/10.3389/fcell.2021.741046.

[32] Yu LP, Qian WW, Yin GY, Ren YX, Hu ZY. MRI assessment of lumbar intervertebral disc degeneration with lumbar degenerative disease using the Pfirrmann grading systems. PLoS One 2012;7(12):e48074. https://doi.org/10.1371/journal.pone.0048074.

[33] Chen Z, Yang X, Zhou Y, Liang Z, Chen C, Han C, et al. Dehydrocostus Lactone Attenuates the Senescence of Nucleus Pulposus Cells and Ameliorates Intervertebral Disc Degeneration via Inhibition of STING-TBK1/NF-κB and MAPK Signaling. Front Pharmacol 2021;12:641098. https://doi.org/10.3389/fphar.2021.641098.

[34] Gonzalez CD, Resnik R, Vaccaro MI. Secretory Autophagy and Its Relevance in Metabolic and Degenerative Disease. Front Endocrinol (Lausanne) 2020;11:266. https://doi.org/10.3389/fendo.2020.00266.

[35] Lu R, He Z, Zhang W, Wang Y, Cheng P, Lv Z, et al. Oroxin B alleviates osteoarthritis through anti-inflammation and inhibition of PI3K/AKT/mTOR signaling pathway and enhancement of autophagy. Front Endocrinol (Lausanne) 2022;13:1060721. https://doi.org/10.3389/fendo.2022.1060721.

[36] Rabinowitz JD, White E. Autophagy and metabolism. Science 2010;330(6009): 1344–8. https://doi.org/10.1126/science.1193497.

[37] Zhai C, Cheng J, Mujahid H, Wang H, Kong J, Yin Y, et al. Selective inhibition of PI3K/Akt/mTOR signaling pathway regulates autophagy of macrophage and vulnerability of atherosclerotic plaque. PLoS One 2014;9(3):e90563. https://doi.org/10.1371/journal.pone.0090563.

[38] Molladavoodi S, McMorran J, Gregory D. Mechanobiology of annulus fibrosus and nucleus pulposus cells in intervertebral discs. Cell Tissue Res 2020;379(3):429–44. https://doi.org/10.1007/s00441-019-03136-1.

[39] Guterl CC, See EY, Blanquer SB, Pandit A, Ferguson SJ, Benneker LM, et al. Challenges and strategies in the repair of ruptured annulus fibrosus. Eur Cell Mater 2013;25:1–21. https://doi.org/10.22203/ecm.v025a01.

[40] Sharifi S, Bulstra SK, Grijpma DW, Kuijer R. Treatment of the degenerated intervertebral disc; closure, repair and regeneration of the annulus fibrosus. J Tissue Eng Regen Med 2015;9(10):1120–32. https://doi.org/10.1002/term.1866.

[41] Hemati K, Pourhanifeh MH, Fatemi I, Hosseinzadeh A, Mehrzadi S. Anti-Degenerative Effect of Melatonin on Intervertebral Disc: Protective Contribution against Inflammation, Oxidative Stress, Apoptosis, and Autophagy. Curr Drug Targets 2022;23(7):711–8. https://doi.org/10.2174/1389450123666220114151654.

[42] Zhang Y, Sun Z, Liu J, Guo X. Advances in susceptibility genetics of intervertebral degenerative disc disease. Int J Biol Sci 2008;4(5):283–90. https://doi.org/10.7150/ijbs.4.283.

[43] Xie S, Zhao C, Chen W, Li G, Xiong Z, Tang X, et al. Recombinant human bone morphogenetic protein 2 and 7 inhibit the degeneration of intervertebral discs by blocking the Puma-dependent apoptotic signaling. Int J Biol Sci 2021;17(9): 2367–79. https://doi.org/10.7150/ijbs.56823.

[44] Madhu V, Guntur AR, Risbud MV. Role of autophagy in intervertebral disc and cartilage function: implications in health and disease. Matrix Biol 2021;100-101: 207–20. https://doi.org/10.1016/j.matbio.2020.12.002.

[45] Tang Z, Hu B, Zang F, Wang J, Zhang X, Chen H. Nrf2 drives oxidative stress-induced autophagy in nucleus pulposus cells via a Keap1/Nrf2/p62 feedback loop to protect intervertebral disc from degeneration. Cell Death Dis 2019;10(7):510. https://doi.org/10.1038/s41419-019-1701-3.

[46] Leung VY, Aladin DM, Lv F, Tam V, Sun Y, Lau RY, et al. Mesenchymal stem cells reduce intervertebral disc fibrosis and facilitate repair. Stem Cells 2014;32(8): 2164–77. https://doi.org/10.1002/stem.1717.

[47] Au TYK, Lam TK, Peng Y, Wynn SL, Cheung KMC, Cheah KSE, et al. Transformation of resident notochord-descendent nucleus pulposus cells in mouse injury-induced fibrotic intervertebral discs. Aging Cell 2020;19(11):e13254. https://doi.org/10.1111/acel.13254.

[48] Pathak SK, Kumar N, Bagtharia P. Alkaptonuria and multilevel intervertebral disc calcification. Joint Bone Spine 2020;87(3):259. https://doi.org/10.1016/j.jbspin.2020.01.004.

[49] Francisco V, Pino J, González-Gay M, Lago F, Karppinen J, Tervonen O, et al. A new immunometabolic perspective of intervertebral disc degeneration. Nat Rev Rheumatol 2022;18(1):47–60. https://doi.org/10.1038/s41584-021-00713-z.

[50] Zhang GZ, Deng YJ, Xie QQ, Ren EH, Ma ZJ, He XG, et al. Sirtuins and intervertebral disc degeneration: Roles in inflammation, oxidative stress, and mitochondrial function. Clin Chim Acta 2020;508:33–42. https://doi.org/10.1016/j.cca.2020.04.016.

[51] Li Z, Wang X, Pan H, Yang H, Li X, Zhang K, et al. Resistin promotes CCL4 expression through toll-like receptor-4 and activation of the p38-MAPK and NF-κB signaling pathways: implications for intervertebral disc degeneration. Osteoarthritis Cartilage 2017;25(2):341–50. https://doi.org/10.1016/j.joca.2016.10.002.

[52] Zhang Y, Lu R, Huang X, Yin E, Yang Y, Yi C, et al. Circular RNA MELK Promotes Chondrocyte Apoptosis and Inhibits Autophagy in Osteoarthritis by Regulating MYD88/NF-κB Signaling Axis through MicroRNA-497-5p. Contrast Media Mol Imaging 2022;2022:7614497. https://doi.org/10.1155/2022/7614497.

[53] Liu ZM, Lu CC, Shen PC, Chou SH, Shih CL, Chen JC, et al. Suramin attenuates intervertebral disc degeneration by inhibiting NF-κB signalling pathway. Bone Joint Res 2021;10(8):498–513. https://doi.org/10.1302/2046-3758.108.Bjr-2020-0041.R3.

[54] Lv F, Yang L, Wang J, Chen Z, Sun Q, Zhang P, et al. Inhibition of TNFR1 Attenuates LPS Induced Apoptosis and Inflammation in Human Nucleus Pulposus Cells by Regulating the NF-KB and MAPK Signalling Pathway. Neurochem Res 2021;46(6): 1390–9. https://doi.org/10.1007/s11064-021-03278-1.

[55] Zhang GZ, Liu MQ, Chen HW, Wu ZL, Gao YC, Ma ZJ, et al. NF-κB signalling pathways in nucleus pulposus cell function and intervertebral disc degeneration. Cell Prolif 2021;54(7):e13057. https://doi.org/10.1111/cpr.13057.

[56] Ge Y, Huang M, Yao YM. Autophagy and proinflammatory cytokines: Interactions and clinical implications. Cytokine Growth Factor Rev 2018;43:38–46. https://doi.org/10.1016/j.cytogfr.2018.07.001.

[57] Yang S, Zhang F, Ma J, Ding W. Intervertebral disc ageing and degeneration: The antiapoptotic effect of oestrogen. Ageing Res Rev 2020;57:100978. https://doi.org/10.1016/j.arr.2019.100978.

[58] Zhang X, Huang WJ, Chen WW. TGF-β1 factor in the cerebrovascular diseases of Alzheimer's disease. Eur Rev Med Pharmacol Sci 2016;20(24):5178–85.

[59] Dropmann A, Dediulia T, Breitkopf-Heinlein K, Korhonen H, Janicot M, Weber SN, et al. TGF-β1 and TGF-β2 abundance in liver diseases of mice and men. Oncotarget 2016;7(15):19499–518. https://doi.org/10.18632/oncotarget.6967.

[60] Kyritsi K, Kennedy L, Meadows V, Hargrove L, Demieville J, Pham L, et al. Mast Cells Induce Ductular Reaction Mimicking Liver Injury in Mice Through Mast Cell-Derived Transforming Growth Factor Beta 1 Signaling. Hepatology 2021;73(6): 2397–410. https://doi.org/10.1002/hep.31497.

[61] Li H, Li W, Liang B, Wei J, Yin D, Fan Q. Role of AP-2α/TGF-β1/Smad3 axis in rats with intervertebral disc degeneration. Life Sci 2020;263:118567. https://doi.org/10.1016/j.lfs.2020.118567.

[62] Morita W, Snelling SJB, Wheway K, Watkins B, Appleton L, Carr AJ, et al. ERK1/2 drives IL-1β-induced expression of TGF-β1 and BMP-2 in torn tendons. Sci Rep 2019;9(1):19005. https://doi.org/10.1038/s41598-019-55387-1.

[63] Cui L, Wei H, Li ZM, Dong XB, Wang PY. TGF-β1 aggravates degenerative nucleus pulposus cells inflammation and fibrosis through the upregulation of angiopoietin-like protein 2 expression. Eur Rev Med Pharmacol Sci 2020;24(23):12025–33. https://doi.org/10.26355/eurrev_202012_23991.